Figure S1. Generation of DA neuron-specific VPS35 knock-out (VPS35$^{DAT-Cre}$) mice, related to Figure 1.

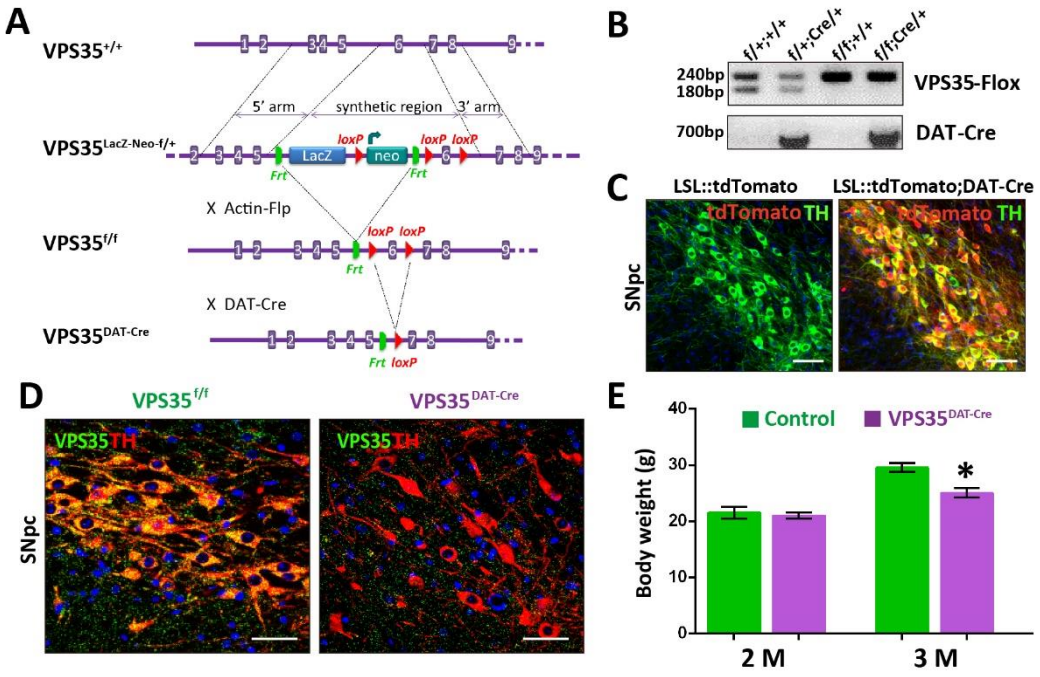

(A) Schematic of generation of DA neuron-specific VPS35 knock-out (VPS35$^{DAT-Cre}$) mice. First panel, genomic structure of the VPS35; second panel, VPS35 allele after homologous recombination in ES cells; third panel, targeted VPS35 allele without the LacZ-Neo cassette; forth panel, targeted VPS35 allele without exon 6 (VPS35DA cKO). Frt, Flp recognition target; neo, Neomycin resistance cassette. **(B)** Genotyping of VPS35$^{DAT-Cre}$ mice and control littermates. Genomic DNA was isolated from mouse tail for PCR with indicated primers. Cre primers generate 750-bp products. VPS35-Flox primers generate 180-bp products in wild type, or 240-bp products in floxed allele. The genotype DAT-Cre; VPS35-loxP/loxP was considered as the conditional knockout (VPS35$^{DAT-cre}$). **(C)** DAT-Cre recombinase expressed in DA neurons. Rosa::LSL::tdTomato mice were crossed with or without DAT-Cre mice. Immunofluorescence for TH (Green) and tdTomato (Red) in coronal sections from Rosa::LSL::tdTomato and Rosa::LSL::tdTomato;DAT-Cre shows in C. Scale bars: 20 μm. **(D)** Decrease of VPS35 expression in DA neurons in VPS35$^{DAT-Cre}$ mice. Dual immunofluorescence for VPS35 (Green) and TH (Red) in coronal sections. Scale bars: 20 μm. **(E)** Slight reduction of body weight in VPS35$^{DAT-Cre}$ mice. Body weight was measured in 2-M old and 3-M old VPS35$^{DAT-Cre}$ mice (n = 6) and control littermates (n = 8). Data are presented as mean ± SEM. * $p < 0.05$.

Figure S2. Decreased Mfn2 in VPS35-deficient neuroblastomal cells and normal Mfn2 transcription in aged VPS35$^{+/-}$ brain areas, related to Figure 2.

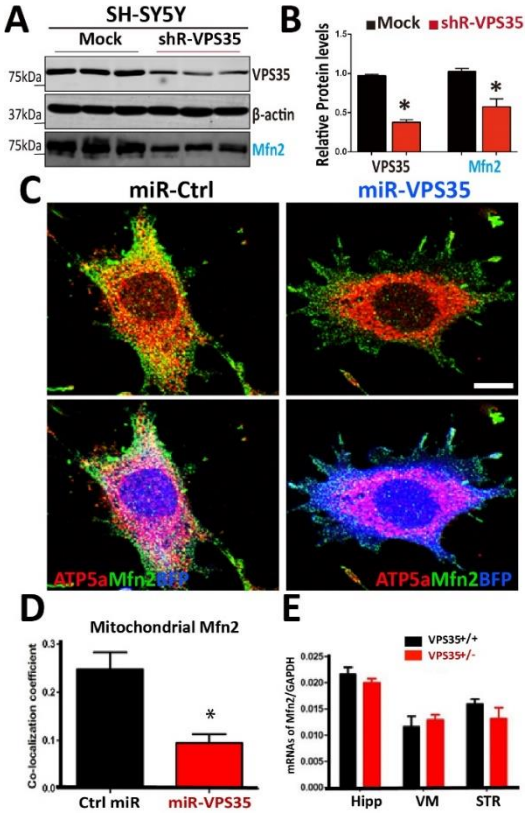

(A-B) Immunoblot analysis of Mfn2 levels in SH-SY5Y cells transfected with indicated plasmids. A, Representative blots; B, Quantification of Mfn2 levels (mean ± SEM, n = 3; *$p < 0.05$). **(C-D)** Mitochondrial Mfn2 was reduced in NLT cells expressing miR-VPS35. Transfected NLT cells were fixed and subjected to immunostaining analysis using indicated antibodies. Mitochondria were labeled by anti-ATP5a antibody. C, Representative images; Scale bars: 5 μm. D, Quantification of mitochondrial-Mfn2 (mean ± SEM; n = 20 cells; *$p < 0.05$). **(E)** No difference in Mfn2 mRNA between VPS35$^{+/+}$ and $^{+/-}$ mice in different brain regions. The mRNA of 12-M old mice was analyzed by real time PCR analysis.

Figure S3. Mitochondrial fragmentation in VPS35-deficient neuroblastomal cells and rescue of shR-VPS35-induced mitochondrial fragmentation by shRNA-resistant VPS35, related to Figure 3.

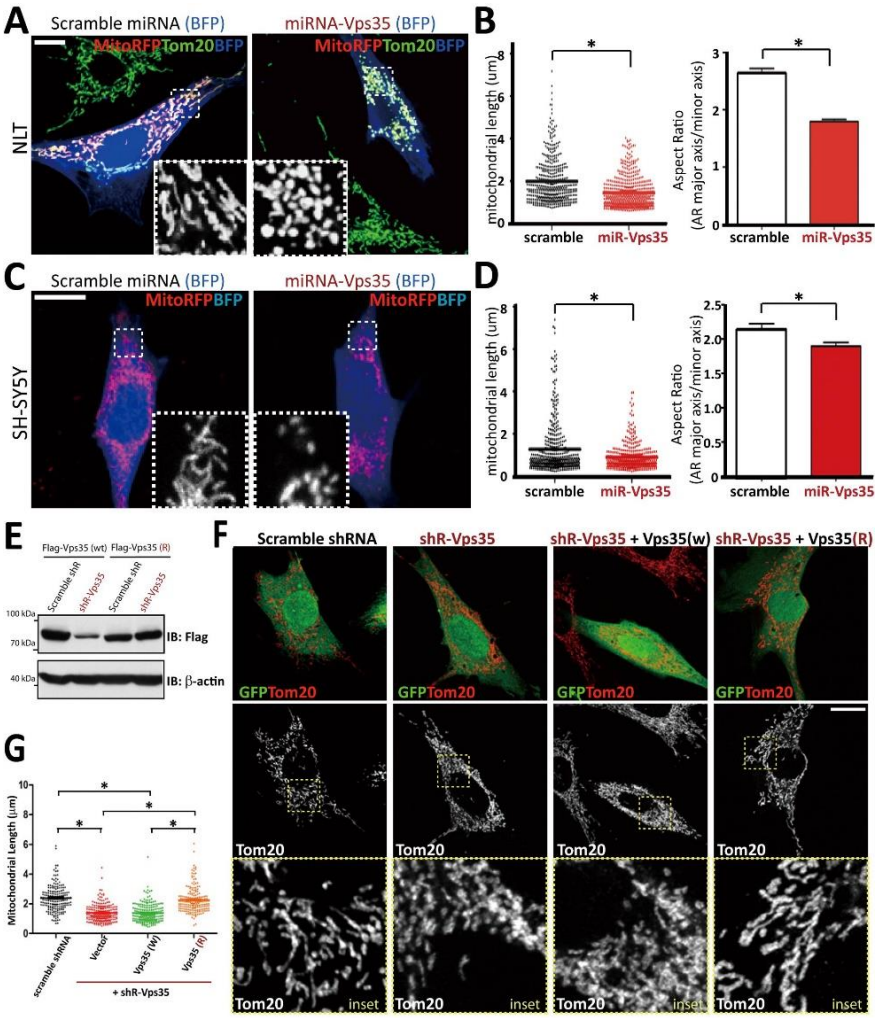

(A-D) NLT and SH-SY5Y cells were transfected with miRNA-VPS35 or scramble control (marked by eBFP) and examined for mitochondrial morphology. A and C, Representative images; B and D, Quantitative data. *$p < 0.05$; Scale bars: 5 μm. **(E)** Restoration of VPS35 protein by co-expressing shRNA-resistant, but not shRNA-sensitive, VPS35, in SH-SY5Y cells. SH-SY5Y cells were transfected with indicated plasmids. Cell lysates were subjected to Western blot analysis. **(F-G)** Rescue of shRNA-VPS35-induced mitochondrial fragmentation in NLT cells by shRNA-resistant VPS35. F, Representative images. Areas in squares are enlarged in bottom panels. Bar, 5 μm. G, Quantification of mitochondrial lengths as column scatter (n = 3 independent experiments, with > 200 mitochondria per experiment; *$p < 0.05$).

Figure S4. Abnormal and dysfunctional mitochondria in VPS35$^{+/-}$ midbrains, related to Figure 4.

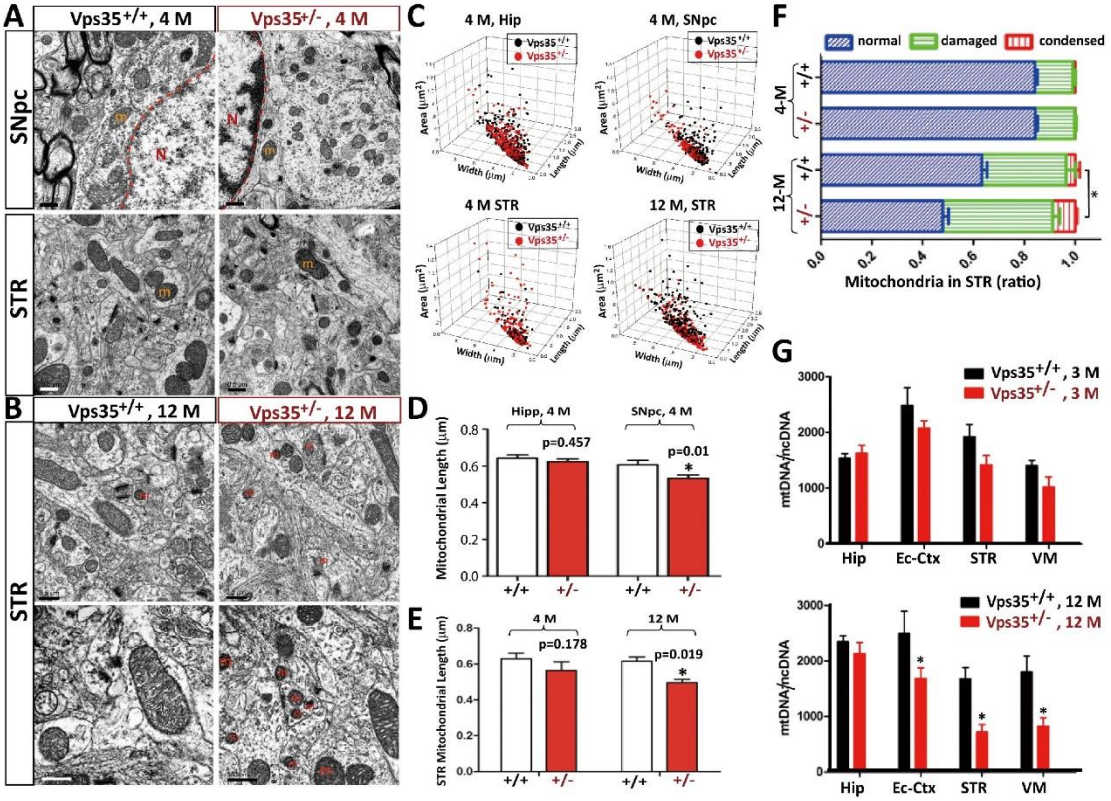

(A-E) Reduced mitochondrial length in VPS35$^{+/-}$ SNpc and STR by transmission electron microscopic (TEM) analysis. A and B, Representative TEM images. Scale bars, 0.5 μm. C, 3D scatter plot graphs of the distribution of area/width/length of individual mitochondria. D and E, Quantitative analysis of TEM data. Data are presented as mean ± SEM; n > 200 mitochondria; *p* values are indicated in the figure. **(F)** The proportion of normal, damaged or condensed/aggregated mitochondria in 4 or 12-M old VPS35$^{+/-}$ STR. Data are presented as mean ± SEM; n = 3 mice/genotype; **p* < 0.05. **(G)** Decreased mtDNA/nuDNA ratio in aged, but not young, entorhinal cortex (Ec-ctx), STR, and VM. Relative copy numbers of mtDNA and ncDNA were calculated from the DCt by qPCR. Data are presented as mean ± SEM; n = 3; **p* < 0.05.

Figure S5. Increased Mfn2 ubiquitination and degradation in VPS35-deficient cells, related to Figure 5.

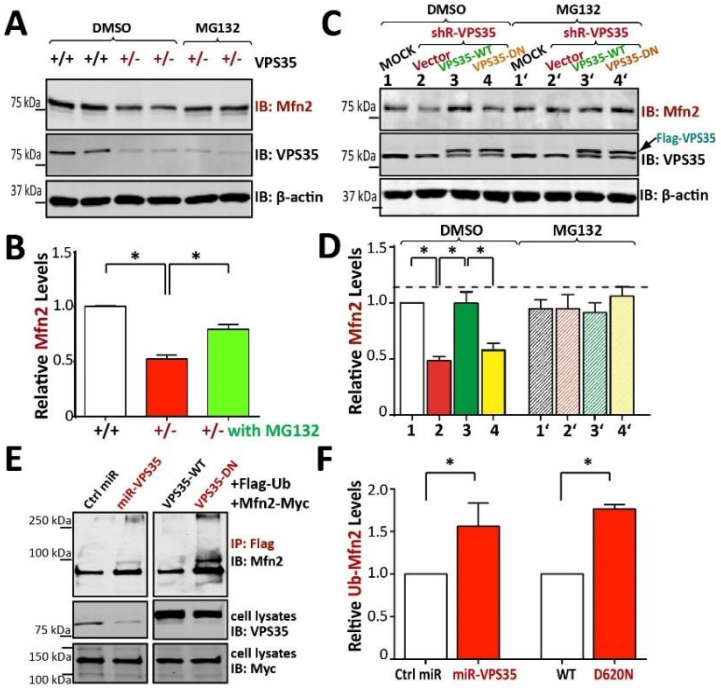

(A-B) Restoration of Mfn2 levels in VPS35$^{+/-}$ neurons by MG132. Neurons were treated with 30 mM MG132 for 6 hrs and blotted for different proteins (A). Mfn2 level is quantified in B (mean ± SEM; n = 5; *p < 0.05). **(C-D)** Restoration of Mfn2 levels in VPS35-deficeint SH-SY5Y cells by MG132 and expressing VPS35-WT, but not VPS35-D620N. C, Representative blots; D, Quantitative data (normalized by b-actin loading and Mock control) (mean ± SEM; n = 3; *p < 0.05). **(E-F)** Increased Mfn2-ubiquitination in VPS35-deficient (miR-VPS35) and VPS35 mutation (VPS35-DN) SH-SY5Y cells. Mfn2 was immunoprecipitated from lysates of transfected SH-SY5Y cells, and the resulting complex was subjected to immunoblotting analyses using indicated antibodies. E, Representative blots; F, Quantification of ubiquitinated Mfn2 (Ub-Mfn2). Level in control cells was set as 1. Data are shown as mean ± SEM (n = 3; *p <0.05).

Figure S6. Restoration of Mfn2 and mitochondrial deficits by suppressing Mul1 expression in VPS35-deficient NLT and neurons, related to Figure 7.

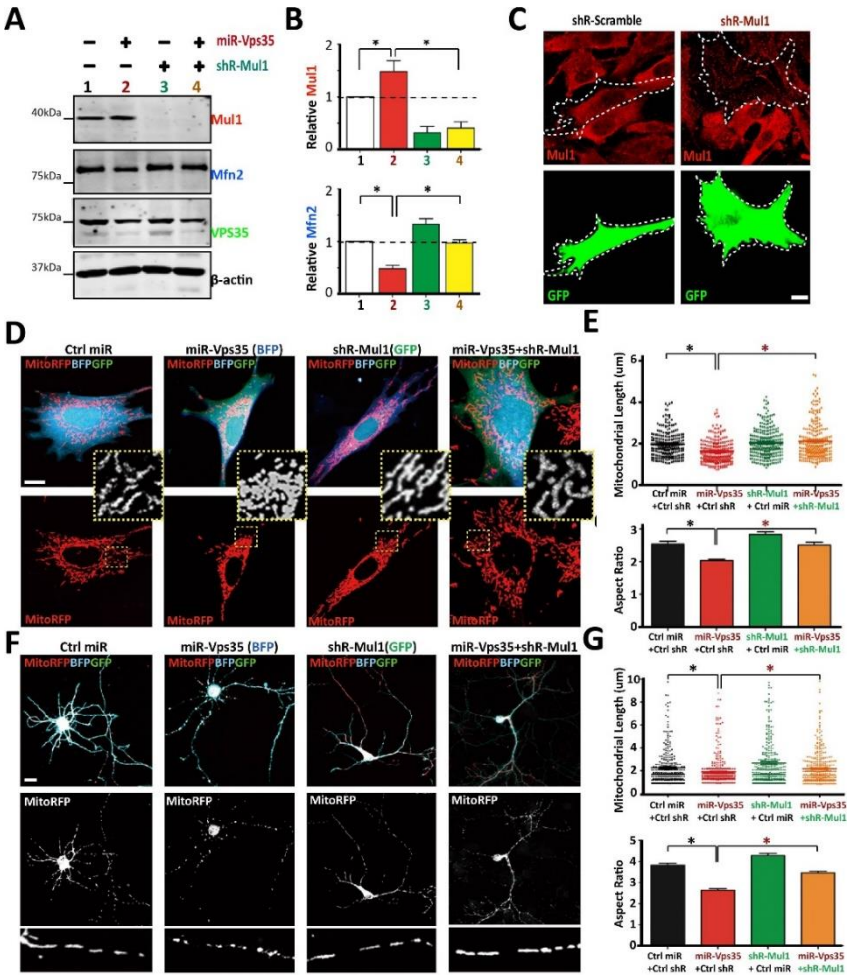

(A-B) Immunoblot analysis of Mul1 and Mfn2 levels in SH-SY5Y cells transfected with indicated plasmids. A, Representative blots; B, Quantification of Mul1 and Mfn2 levels (normalized by untransfected cells). **(C)** Endogenous Mul1 level was suppressed by shR-Mul1-1 in transfected NLT cells. Transfected cells are marked by white dash lines. Bar, 5 μm. **(D-E)** Mitochondrial fragmentation in miRNA-VPS35-expressing NLT cells was mitigated by co-expressing shRNA-Mul1. D, Representative confocal images. Scale bar, 5 μm. E, Quantitative data of mitochondrial length are shown as grouped column scatter and aspect ratio. Data are presented as mean ± SEM (n = 200 mitochondria from 10 different cells; *$p < 0.05$). **(F-G)** Mitochondrial fragmentation in VPS35-deficient neurons was ameliorated by expressing shRNA-Mul1. F, Representative confocal images. Higher magnification images are shown in bottom panels. Scale bar, 10 μm. Quantitative data of mitochondrial length is shown as grouped column scatter and aspect ratio. Data are presented as mean ± SEM (n = 200 mitochondria from 10 different cells; *$p < 0.05$).

Figure S7. Restoration of mitochondrial fragmentation and DA neuron loss by suppressing Mul1 expression in VPS35-D620N expressing SNpc, related to Figure 7.

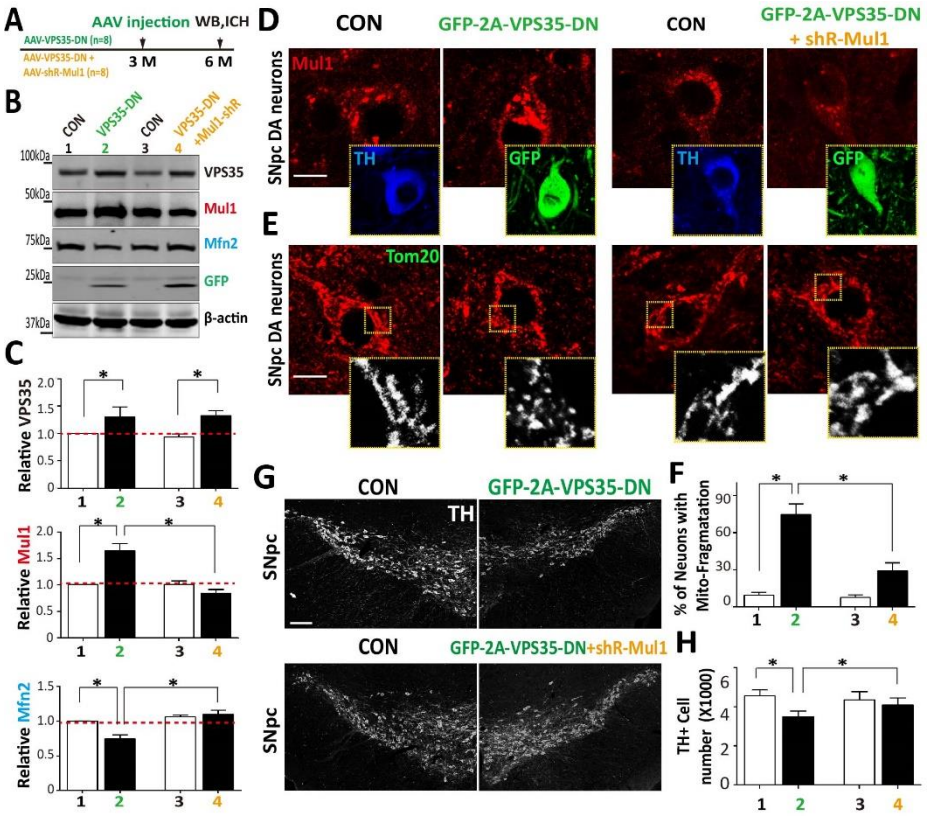

(A) Schematic of AAV injection strategy. AAV5 coated GFP-2A-VPS35-D620N and GFP-shR-Mul1 were stereotactically injected into the SNpc of 3-M old WT mouse. Three months post-injection, coronal brain sections and ventral midbrain homogenates were collected and subjected to immunohistochemical staining and Western blot analyses, respectively. **(B)** Representative Western blots of homogenates of ventral midbrain derived from the ipsilateral (VPS35-DN or VPS35-DN+shR Mul1) and contralateral (CON) hemispheres. **(C)** Quantification of data from B. Relative VPS35, Mul1 and Mfn2 protein levels were normalized by CON side. Means ± SEM (n = 4) are shown. **(D-F)** Mitochondrial fragmentation in VPS35-D620N overexpression DA neurons (indicated by TH or GFP) were mitigated by co-expressing shRNA-Mul1. Representative images of Mul1 (D) or Tom20 (E) immunostaining in the ipsilateral (VPS35-DN or VPS35-DN+shR Mul1) and contralateral (CON) SNpc (Scale bar = 10 μm). Quantification of percentage of DA neurons with mitochondrial fragmentation is shown in F, **(G-H)** Stereological analysis of TH-positive dopaminergic neurons in SNpc. G, Representative images of TH immunostaining in the SNpc (Scale bar = 200 μm). Quantification analysis (mean ± SEM, n = 4 animals/group) is presented in H. *$p < 0.05$.

Supplemental Experimental Procedures

Generation of Vps35$^{DAT\text{-}Cre}$ mice, crossing and genotypying

VPS35$^{DAT\text{-}Cre}$ mice were newly generated by crossing floxed allele of VPS35 (VPS35$^{f/f}$) with DAT-Cre mice. The VPS35$^{f/f}$ mice were generated by injecting VPS35$^{tm1a(EUCOMM)Hmgu}$ ES cells (KO-first promoter-driven reporter-tagged insertion with conditional potential, purchased from International Mouse Phenotyping Consortium (IMPC), Germany) into the inner cell mass of C57BL/6J blastocysts. A floxed allele of the VPS35 gene contains loxP sites flanking exon 6 (Fig. S1G). The injected blastocysts were then implanted into the uterus of pseudo-pregnant foster mothers for further development. The LacZ-Neo cassette flanked by Flp recombinase recognition site (Frt) was removed by crossing mice carrying the VPS35-neo-lacZ-flox allele to FLPe transgenic mice (B6;J-Tg(ACTFLPe)9205Dym/J) (Jackson Laboratories), which express a Flp recombinase, to generate VPS35-loxP mice. The floxed mice were genotyped by PCR analysis of mouse tail DNA using primer set across the 3' loxP site which are 5'-AACCAGCTCCCAACAAAATG -3' and 5'- AAATGTGAGTGGGACCAAGC -3'. The DAT-Cre mice, obtained from Dr. Xiaoxi Zhuang, University of Chicago, and Dr. Philip Wang, Georgia Regents University), specifically express Cre recombinase in DA neurons (Fig. S1I) (Zhuang et al., 2005). The genotyping primers for DAT-Cre were 5'- GCCTGCATTACCGGTCGATGCAACGA -3' and 5'- GTGGCAGATGGCGCGGCAACACCATT -3'. The control mice for VPS35$^{DAT\text{-}Cre}$ were VPS35$^{f/f}$ littermates for each experiment.

Behavior tests

All behavioral experiments were conducted in the light phase from 16:00 to 18:00 hr. Animals were brought into the testing room at least 60 min before the start of behavioral experiments. To evaluate a mouse's motor function and muscle strength, mouse was placed its forelimbs on a tension bar and pulled the mouse back gently until it released the bar. Grip strength was determined by a digital grip-strength meter (Animal Grip Strength System, San Diego Instruments). Mice were placed in a transparent glass walled enclosure (20 cm in height and 14 cm in diameter) for the cylinder observational test. During the 2 min observational trial, the number of rears was counted using a hand counter. A rear is defined as a vertical movement with both forelimbs off the floor so that the mouse is standing only on its hindlimbs (Fleming et al., 2013). The vertical pole test was

performed as previously described (Matsuura et al., 1997). Briefly, the mouse was placed head-upward on the top of a vertical rough-surfaced pole (diameter 9 mm; height 60 cm) and the time until it descended to the floor was recorded with a maximum duration of 120 s. The Open-field test was performed in an arena of 50cm x 50cm at 20cm of height. Mice, placed in the center of the open-field, were allowed to explore the arena undisturbed for 10 min after which they were removed. The arena was cleaned with 70% ethanol between each animal. Video analysis and data acquisition were obtained with Noldus tracking software (Ethovision XT, 7.0).

Cloning, RNAi, and mutagenesis

VPS35 cDNA (a kind gift from Dr. Tae Wan Kim, Columbia University) was sub-cloned into pEGFP-N1 (Clontech) as described previously (Zhu et al., 2007). VPS35-D620N mutations were introduced by PCR-mediated site-directed mutagenesis and sequenced to confirm its integrity. The Mul1 cDNA was obtained from DNASU and inserted into the KpnI and XhoI sites of pEGFP-N1. The mito-RFP plasmids were obtained from Addgene. The miRNA-VPS35-EmGFP expression vector was described previously (Xia et al., 2013). The miRNA-VPS35-eBFP was constructed by replacing the EmGFP with eBFP sequence from pBad-eBFP2. The shRNA-Mul1 RNAi vector was generated by the pSuper vector system. The target sequences, 5′-AGGTGTAAATGTGGAACGTTA-3′ for miR-VPS35, and 5′- GAGCTGTGCGGTCTGTTAA -3′ for shR-Mul1, were designed using web-based Block-iT program (Invitrogen), respectively.

Immunofluorescence staining and confocal imaging analyses

Cells plated on coverslips in 24-well plates and fixed in 4% paraformaldehyde for 15 min, permeabilized with 0.2% saponin, and blocked with 10% normal goat serum and 0.1% saponin prior to incubation with primary antibodies overnight: mouse anti-TH (Sigma,1:20,000), rabbit anti-Tom20 (Santa Cruz, 1:2000), rabbit anti-Mul1 (thermo, 1:500), rabbit anti-VPS35 (1:1000), mouse anti-ATP5A (Abcam, 1:500), and rabbit anti-Mfn2 (Abcam, 1:500). Cells were then labeled with appropriate secondary antibody raised in goat (Invitrogen). Images were taken with the LSM510 (Zeiss) confocal microscope by using the 20×/0.5 EC Plan-Neofluar objective or the 63×/1.4 Oil Plan-Apochromat objective. Excitation and acquisition parameters were constrained across all paired comparisons. For fluorescent quantification, morphometric measurements of images were performed using Image-Pro Plus software (MediaCybernetics).

Mitochondrial morphology quantification was conducted by the Mito-Morphology Macro

(Dagda et al., 2009) through ImageJ software (National Institutes of Health). In brief, images of 20 cells from random view field of each group were first processed with a median filter to obtain isolated and equalized fluorescence, then individual mitochondrial were analyzed for the lengths of major and minor axes. The Aspect Ratio (AR) was derived from major axis/minor axis. The AR minimal value of 1 corresponds to the perfect circle, and this value elevates when the mitochondrial become elongated.

Cell culture and transfection

NLT cells and SH-SY5Y cells were grown in DMEM/F-12 (Hyclone) with 5% fetal bovine serum (Invitrogen) at 37 ℃ with 5% CO2. Transfection was performed using polyethylenimine (Aldrich cat. no. 40,872-7) as described (Wu et al., 2012). Plasmids were expressed for 48–72 h prior to experimental processing.

Mitochondrial fractions

Striatum and ventral midbrain (VM) tissue from WT and VPS35$^{+/-}$ mice were resuspended in mitochondrial isolation buffer (220 mM mannitol, 75 mM sucrose, 30mM Tris, 1mM EDTA, 0.5mM PMSF, pH 7.6) and homogenized by passing through a 27-gauge needle 8 times. After incubation on ice for 15 min, nuclei and unbroken cells were removed by centrifugation at 740 g for 10 min. The supernatant was centrifuged at 9,000 g for 10 min to obtain the cytosolic fraction (supernatant). The pellet was subjected to two additional rounds of homogenization and differential centrifugation. The mitochondrial fraction was pelleted by the final centrifugation at 14,000 g for 20 min. Protein concentrations were measured by BCA kit from Pierce.

Western blot analysis

Cells or brains were homogenized with lysis buffer (50 mM Tris-HCl (pH 7.4), 150 mM NaCl, 0.5% sodium deoxycholate, 1% Triton X-100, 0.1% SDS) containing protease and phosphatase inhibitor cocktails (Pierce). Cell and tissue lysates were centrifuged at 14 000 g for 20 min at 4 ℃. To obtain the insoluble fraction, Triton X-100-insoluble pellets were solubilized in buffer containing 2% SDS, 8M urea, 50 mM Tris-HCl (pH 7.4) and complete protease inhibitors (Roche). Equivalent proteins as determined by BCA assay (Pierce Biotechnology) were resolved by SDS-PAGE and subjected to western blot analysis with appropriate primary antibodies: rabbit anti-VPS35 (1:10,000), mouse anti-TH (Sigma; 1:40,000), mouse anti-β-actin (Sigma; 1:10,000), mouse anti-LRRK2 (Sigma, 1:2,000), rabbit anti-Pink1(abcam, 1:1,000), rabbit anti-Parkin (abcam, 1:1,000), rabbit anti-Drp1

(Novus Bio, 1:2,000), rabbit anti-Mfn2(cell sig, 1:2,000), mouse anti-ATP5a (abcam，1:5,000)，rabbit anti-Mul1(abcam, 1:3,000), mouse anti-Ubiquitin (Santa Cruz, 1:1,000). Acquired images were subjected to densitometric quantitation using NIH ImageJ software.

Immunoprecipitation analysis in denaturing condition

SH-SY5Y cells were transiently transfected with plasmids expressing shRNA or miRNA and ubiquitin. 48 hr post-infection, cells were denatured in 2% SDS buffer (2% SDS, 150 mM NaCl, 10 mM Tris-HCl, pH 8.0 with 2mM sodium orthovanadate, 50 mM sodium fluoride, and protease inhibitors) and diluted with dilution buffer (10 mM Tris-HCl, pH 8.0, 150 mM NaCl, 2 mM EDTA, 1% Triton). The mixtures were subjected to the IP assay with anti-Mfn2 antibody and protein A sepharose overnight (Roch).

Electron microscopy

Electron microscopic (EM) analysis of mitochondria was performed as described previously (Wu et al., 2012). 4- and 12-M old animals were perfused with 100 mL of 4% paraformaldehyde with 2% glutaraldehyde in 100 mM sodium phosphate buffer at pH 7.4. Brains were removed and post-fixed in the same perfusion fixative overnight. A piece of the Hip/STR/SNpc was excised from the brain, which was post-fixed in 2% osmium tetroxide in NaCac, stained en bloc with 2% uranyl acetate, dehydrated with a graded ethanol series and embedded in Epon-Araldite resin. Thin sections were cut with a diamond knife on a Leica EM UC6 ultramicrotome (Leica Microsystems, *Inc*., Bannockburn, IL), collected on copper grids and stained with uranyl acetate and lead citrate. Samples were imaged in a JEM 1230 transmission electron microscope (JEOL USA Inc., Peabody, MA) at 110 kV with an UltraScan 4000 CCD camera & First Light Digital Camera Controller (Gatan Inc., Pleasanton, CA). Thirty randomly selected EM images per animal were analyzed by blinded investigator with Image J software (NIH). Mitochondria were subclassified as normal, damaged or abnormally condensed groups by the morphology as described previously (Ramonet et al., 2011). The length of each mitochondria was measured within each image using Image-Pro Plus software (MediaCybernetics).

Quantification of mitochondrial DNA (mtDNA) copy number by qPCR

The whole DNA was isolated with the QIAamp DNA Mini Kit according to the manufacturer's protocol. The contents of mtDNA and nuclear DNA (ncDNA) were measured by real-time quantitative PCR using specific primers for the mitochondrion gene and the nuclear gene

[platelet/endothelial cell adhesion molecule 1 (Pecam1)]. In brief, the primers for qPCR analysis for mtDNA were mtF(5'-CCT ATC ACC CTT GCC ATC AT-3') and mtR (5'-GAG GCTGTT GCT TGT GTG AC-3'); for ncDNA were ncF(5'-ATG GAA AGC CTG CCA TCA TG-3') and ncR(5'-TCC TTG TTG TTC AGC ATC AC-3'). qPCR was performed in Bio-Rad PTC-200 w/Chromo4 Real Time PCR system using the following cycling parameters: 95^{o}C (5min), and 40 cycles of 95^{o}C (15s), 60^{o}C (1 min). The mtDNA copy number is calculated from the difference in threshold cycle numbers (the delta cycle threshold) of mtDNA and ncDNA.

High-Performance Liquid Chromatography

The dopamine (DA) levels in the striatum tissues were determined using a modified method (Yin et al., 2013). The striatum tissue from contralateral and ipsilateral side were weighed and then homogenized in 0.2 M ice-cold perchloric acid (0.5 ml / 100mg wet tissue, 100ng isoproterenol (ISO)/100mg of wet tissue was added as an internal control). Cell membranes were disrupted using a sonicator in an ice bath and centrifuged at 20,000g for 10 min at 4 ℃. The supernatants were filtered through 0.44 μm Millipore filter and injected into the HPLC column (Eicompak SC3ODS, 3.0* 100mm) for analysis by using high-performance liquid chromatography (HPLC) with electrochemical detection (Eicom, USA). The mobile phase contained 110 mM citrate buffer/100 mM EDTA/70 mM sodium octane sulfonate (SOS) and 20% (v/v) methanol. Flow rate was at 320 ul/min. DA levels were calculated using a DA standard (Dopamine hydrochloride, Sigma) and normalized to the sample dopamine levels. DA levels were expressed as ng/mg protein.

Supplemental References

Dagda, R.K., Cherra, S.J., 3rd, Kulich, S.M., Tandon, A., Park, D., and Chu, C.T. (2009). Loss of PINK1 function promotes mitophagy through effects on oxidative stress and mitochondrial fission. The Journal of biological chemistry *284*, 13843-13855.

Fleming, S.M., Ekhator, O.R., and Ghisays, V. (2013). Assessment of sensorimotor function in mouse models of Parkinson's disease. Journal of visualized experiments : JoVE.

Matsuura, K., Kabuto, H., Makino, H., and Ogawa, N. (1997). Pole test is a useful method for evaluating the mouse movement disorder caused by striatal dopamine depletion. Journal of neuroscience methods *73*, 45-48.

Ramonet, D., Daher, J.P., Lin, B.M., Stafa, K., Kim, J., Banerjee, R., Westerlund, M., Pletnikova, O., Glauser, L., Yang, L., *et al.* (2011). Dopaminergic neuronal loss, reduced neurite complexity and autophagic abnormalities in transgenic mice expressing G2019S mutant LRRK2. PLoS One *6*, e18568.

Wu, H., Lu, Y., Shen, C., Patel, N., Gan, L., Xiong, W.C., and Mei, L. (2012). Distinct roles of muscle and motoneuron LRP4 in neuromuscular junction formation. Neuron *75*, 94-107.

Xia, W.F., Tang, F.L., Xiong, L., Xiong, S., Jung, J.U., Lee, D.H., Li, X.S., Feng, X., Mei, L., and Xiong, W.C. (2013). Vps35 loss promotes hyperresorptive osteoclastogenesis and osteoporosis via sustained RANKL signaling. The Journal of cell biology *200*, 821-837.

Yin, D.M., Chen, Y.J., Lu, Y.S., Bean, J.C., Sathyamurthy, A., Shen, C., Liu, X., Lin, T.W., Smith, C.A., Xiong, W.C., *et al.* (2013). Reversal of behavioral deficits and synaptic dysfunction in mice overexpressing neuregulin 1. Neuron *78*, 644-657.

Zhu, X.J., Wang, C.Z., Dai, P.G., Xie, Y., Song, N.N., Liu, Y., Du, Q.S., Mei, L., Ding, Y.Q., and Xiong, W.C. (2007). Myosin X regulates netrin receptors and functions in axonal path-finding. Nat Cell Biol *9*, 184-192.

Zhuang, X., Masson, J., Gingrich, J.A., Rayport, S., and Hen, R. (2005). Targeted gene expression in dopamine and serotonin neurons of the mouse brain. Journal of neuroscience methods *143*, 27-32.